PNAS
www.pnas.org

Supplementary Information for

Altering gain of the infralimbic to accumbens shell circuit alters economically dissociable decision-making algorithms

Brian M. Sweis[1,2], Erin B. Larson[2], A. David Redish[2]*, Mark J. Thomas[2,3]

[1]Graduate Program in Neuroscience & Medical Scientist Training Program, University of Minnesota, Minneapolis, MN 55455
[2]Department of Neuroscience, University of Minnesota, Minneapolis, MN 55455
[3]Department of Psychology, University of Minnesota, Minneapolis, MN 55455

Correspondence: A. David Redish
Email: redish@umn.edu

This PDF file includes:

Supplementary Materials and Methods
Figs. S1 to S12
Table S1

www.pnas.org/cgi/doi/10.1073/pnas.1803084115

Supplementary Materials and Methods

Animals.

30 C57BL/J6 male mice (wild type), 13 weeks of age, were trained in Restaurant Row. 16 additional behavior-naïve mice were used solely for electrophysiology tests. Mice were single-housed (to protect skull implants) in a temperature- and humidity-controlled environment with a 12-hr-light/12-hr-dark cycle with water ad libitum unless being testing in Restaurant Row in which case only water was ad libitum and food (full nutrition flavored pellets) was task-earned. Mice were food restricted to a maximum of 85% free feeding body weight and trained to earn their entire day's food ration during their 1-hr Restaurant Row testing session. All experiments were approved by the University of Minnesota Institutional Animal Care and Use Committee. Research technicians were blinded to animal conditions. Previous studied using this task yielded reliable behavioral findings with minimal variability in at least sample sizes of n=7 mice per experimental group. Electrophysiology findings from our lab report reliable data from at least n=6 slices.

Surgery.

Animals were anesthetized with a ketamine and xylazine mixture (100 and 10 mg/kg; i.p.) and placed into the stereotaxic frame (Kopf Instruments). Virus AAV8-Syn-Chronos-GFP (University of North Carolina Vector Core Facility) was bilaterally transfected into infralimbic cortex (IL, stereotaxic coordinates adapted from mouse brain atlas: anterior-posterior: +1.65; medial-lateral: ±0.4; dorsal-ventral:−3.2 from bregma) of 7-8 wk old mice. Injections of virus (0.5 µL per injection site) were performed with a 5-µL Hamilton syringe using an UltraMicroPump with SYS-Micro4 controller (World Precision Instruments). After a 5-min delay to reduce solution backflow along the infusion track, the syringe was slowly removed over a 5-min period and incisions were closed using Vetbond (3M). Approximately 1 wk following virus surgery, mice were bilaterally implanted with indwelling optic fibers (200/230 µm core/cladding, 0.66 NA) targeting the accumbens shell (NAcSh, angled: 14 degrees; anterior-posterior: +1.5 mm; medial-lateral: ±1.63; dorsal-ventral: −4.1) using stereotaxic apparatus described above. Light guides were secured to the skull with a dual-cure resin-lonomer (Geristore) that was anchored with two 0.0625-in steel machine screws (amazon.com) with caps (ThorLabs) placed over the top. After approximately 4 wk of recovery, mice began training in behavior while a separate group was yoked and remained housed without behavior training for an equal amount of time before all electrophysiology experiments were conducted in all mice at the same time to match expression level profiles.

Electrophysiology.

Parasagittal slices (240 µm) containing the NAcSh were sliced in an ice-cold solution saturated with 95% O2/5% CO2 containing 75mM sucrose, 87mM NaCl, 2.5mM KCl, 1.25mM NaH2PO4, 26mM NaHCO3, 3mM Na ascorbate, 7mM MgSO4, 0.5mM CaCl2. Slices recovered for at least 60 min in a room-temperature artificial CSF solution saturated with 95% O2/5% CO2 containing 119mM NaCl, 2.5mM KCl, 1.0mM NaH2PO4, 1.3mM MgSO4, 2.5mM CaCl2, 26.2mM NaHCO3, and 11mM glucose. For all electrophysiological recordings, picrotoxin (Sigma-Aldrich, 100µM) was added to block GABAergic neurotransmission. Using an Axon Instruments Multiclamp 700B (Molecular Devices), extracellular field recordings were sampled through a pulled glass pipette electrode filled with aCSF. Recording electrode was placed in NAcSh. Data were filtered at 2 kHz and digitized at 5 kHz via custom Igor Pro software (Wavemetrics). Blue

LEDs (Plexon, 465 nm, 15 mW) were used to drive optical light pulses, delivered into the slice preparation via a 1 meter patch cable (Plexon) connected to a polished bare fiber tip lowered into the field of view and a focal spotlight pulse directed over the tissue surrounding the recording electrode. Pulses were delivered via a Master-8 stimulator (A.M.P.I.). Optically evoked field potentials of the IL-NAcSh circuit were obtained every 15s. Pulse durations ranged from 0.1-4ms. Peak amplitude of the N1 and N2 components of the waveform were calculated from average traces. Pharmacology tests were run by washing in DNQX (Sigma-Aldrich, 1μM, 10μM) or TTX (Tocris, 1μM). %Change in N1 and N2 were measured relative to baseline averages before drugs were washed in or calcium levels changed in the zero-calcium test. Plasticity tests were run by stimulating at a constant stimulus duration determined to elicit a 50% max response for 12.5 min (50 pulses) before delivering either no stimulation (10min), 10 Hz stimulation (10min, 4ms pulses), or 100 Hz stimulation (1s train, 4ms pulses, 4 trains, 10s inter-train-interval) protocols. Following one of these three protocols, regular sampling at the original constant stimulus duration resumed for 37.5 min (150 pulses). %Change in N1 and N2 were measured in the final 50 pulses compared relative to the initial 50 baseline pulses. Synaptic strength assays were carried out by ramping pulses up from 0.1 ms to 1.0 ms in 0.1 ms increments (10 steps) collecting 5 pulses at each step, and then ramping back down, in total collecting 100 pulses taking 25 min. Peak N1 and N2 amplitude pairs were calculated from each stimulus duration step and scatter-plotted against each other. Slope from linear regression was calculated as a metric of strength of synaptic transmission. Slopes were collected before and after plasticity induction protocols to measure change in strength of synaptic transmission as a consequence of slice exposure to no stimulation, 10 Hz, or 100 Hz. Additional mice received either no stimulation, 10 Hz, or 100 Hz in vivo and then were sacrificed 24 hr later for functional connectivity assays to be compared across animals between groups.

Behavior.

Mice underwent 1 week of pellet training prior to the start of being introduced to the Restaurant Row maze. During this period, mice were taken off of regular rodent chow and introduced to a single daily serving of BioServ full nutrition 20 mg dustless precision pellets in excess (5g). This serving consisted of a mixture of chocolate-, banana-, grape-, and plain-flavored pellets. Next, mice (hungry, before being fed their daily ration) were introduced to the Restaurant Row maze 1 day prior to the start of training and were allowed to roam freely for 15 min to explore, get comfortable with the maze, and familiarize themselves with the feeding sites. Restaurants were marked with unique spatial cues. Feeding bowls in each restaurant were filled with excess food on this introduction day.

Task training was broken into 4 stages. Each daily session lasted for 1 hr. At test start, one restaurant was randomly selected to be the starting restaurant where an offer was made if mice entered that restaurant's T-shaped offer zone from the appropriate direction in a counter-clockwise manner. During the first stage (day 1-7), mice were trained for 1 week being given only 1 s offers. Brief low pitch tones (4000 Hz, 500 ms) sounded upon entry into the offer zone and repeated every second until mice skipped or until mice entered the wait zone after which a pellet was dispensed. To discourage mice from leaving earned pellets uneaten, motorized feeding bowls cleared any uneaten pellets upon restaurant exit. Left over pellets were counted after each session and mice quickly learned to not leave the reward site without consuming earned pellets. The next restaurant in the counter-clockwise sequence was always and only the next available restaurant where an offer could be made such that mice learned to run laps encountering offers across all four restaurants in a fixed order serially in a single lap. During the second stage (day 8-12), mice were given offers that ranged from 1 s to 5 s (4000 Hz to 5548 Hz, in 387 Hz steps) for 5 days. Offers were pseudo-randomly selected such that all 5 offer lengths were encountered in 5

consecutive trials before being re-shuffled, selected independently between restaurants. Again, offer tones repeated every second in the offer zone indefinitely until either a skip or enter decision was made. In this stage and subsequent stages, in the wait zone, 500ms tones descended in pitch every second by 387 Hz steps counting down to pellet delivery. If the wait zone was exited at any point during the countdown, the tone ceased and the trial ended, forcing mice to proceed to the next restaurant. Stage 3 (day 13-17) consisted of offers from 1 s to 15 s (4000 Hz to 9418 Hz) for another 5 days. Stage 3 is the first magenta timepoint used in SI Appendix, Fig. S9B-C,H-I,N-O. Stage 4 (day 18-70) offers ranged from 1s to 30s (4000 Hz to 15223 Hz) and lasted until mice showed stable economic behaviors. We used 4 Audiotek tweeters positioned next to each restaurant powered by Lepy amplifiers to play local tones at 70dB in each restaurant. We recorded speaker quality to verify frequency playback fidelity. We used Med Associates 20mg feeder pellet dispensers and 3D-printed feeding bowl receptacles fashioned with mini-servos to control automated clearance of uneaten pellets. Animal tracking, task programming, and maze operation was powered by AnyMaze (Stoelting). Mice were tested at the same time every day in a dim-lit room, were weighed before and after every testing session, and were fed a small post-session ration in a separate waiting chamber on rare occasions as needed to prevent extremely low weights according to IACUC standards (not <85% free-feeding weights).

After 70 consecutive days of testing in Restaurant Row, mice were divided into 3 groups of 10 and received either no stimulation (10 min), 10 Hz stimulation (10 min, 4 ms pulses), or 100 Hz stimulation (1 s train, 4 ms pulses, 4 trains, 10 s inter-train-interval) protocols in the evening 4 hours after Restaurant Row testing completed on day 71 for round 1 of stimulations. Mice were transported to a separate stimulation room and plugged into fiber optic patch cables (Plexon, 1 meter) bilaterally connected to compact magnetic LC blue LEDs (Plexon, 465 nm, 15 mW) on a commutator swivel. Mice resumed regular daily testing in Restaurant Row. On the evening of day 81, mice received round 2 of stimulations, where the 10 Hz and 100 Hz groups swapped stimulation protocols in a cross-over repeated measures design. On the evening of day 93, mice received round 3 of stimulations according to original protocol assignments for 5 consecutive evenings. Mice were tested up until day 106 and retired before being sacrificed for electrophysiological assessments.

Statistical Analysis.

All data were processed in Matlab and statistical analyses were carried out using JMP Pro 13 Statistical Discovery software package from SAS. All data are expressed as mean +/- 1 standard error. Sample size is included in each figure, where electrophysiology data are reported n=slices(mice). Statistical significance was assessed using student's t tests, one-way, two-way, and repeated measures ANOVAs, with post-hoc Tukey t tests correcting for multiple comparisons. Correlations were reported using Pearson correlation r coefficients. Electrophysiology waveforms represent plotted averages from 10-50 consecutive pulsed evoked responses, described in detail in each corresponding figure.

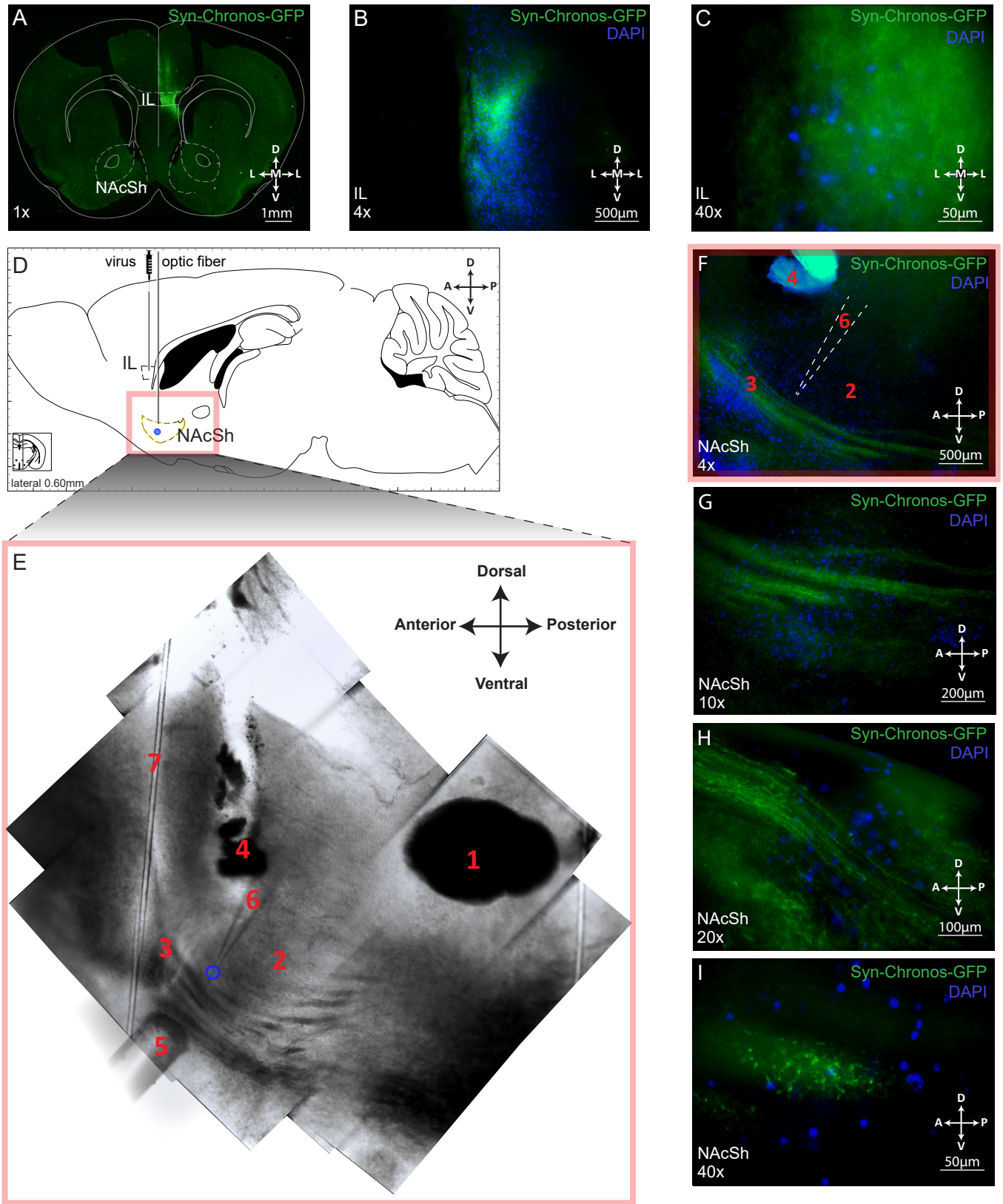

Figure S1. Projection-specific targeting of infralimbic (IL) to accumbens shell (NAcSh) circuit. (A) Coronal section of demonstration mouse unilaterally transfected in IL in the right hemisphere only (mice used in the experiment were bilaterally transfected). IL at the virus transfection site, at 4x (C) and 40x (D). IL cell bodies stained with DAPI. (D) Parasagittal schematic of viral transfection site in IL and optic fiber implantation site in NAcSh (outlined in yellow). Blue dot indicates location of ex vivo recording site. (E) Red box zoom in from (D) depicts light-field microscope image collage from a live recording session in NAcSh under light-field microscope. Representative landmarks and instruments annotated by 1-7. (1) Anterior commissure reference landmark. (2) NAcSh region. (3) High density fiber bundle at the anterior border of the NAcSh. GFP label in fluorescent images in (G) reveal these to be virus-transfected opsin-containing IL afferents. (4) Remnant optic fiber track from in vivo implantation. (5) Working optic fiber tip lowered into the slice for ex vivo illumination. (6) Extra-cellular recording electrode pipette lowered into the slice ex vivo. (7) Cloth harp strand used to hold the slice in place while in the bath. (F) Red box zoom in from (D-E) depicts NAcSh at 4x. Number annotations follow that in (E). Estimated recording pipette location outlined in white. NAcSh cell bodies stained with DAPI. NAcSh imaged at 10x (G), 20x(H), and 40x(I).

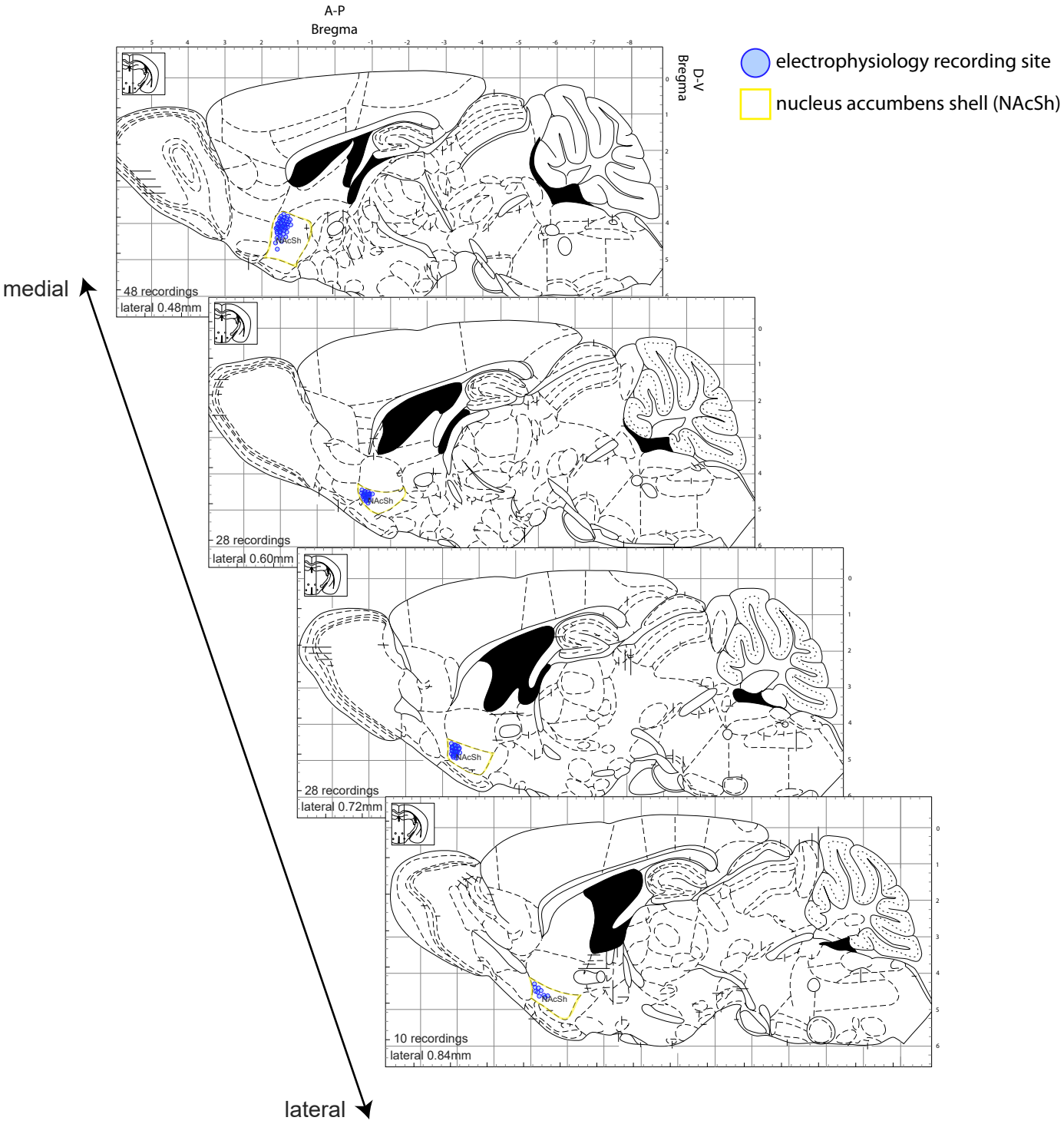

Figure S2. Localization of IL-NAcSh electrophysiology recording measurements. Parasagittal sections taken from the Paxinos mouse brain atlas, with NAcSh outlined in yellow in each section. Translucent blue circles represent recording site locations guided toward the anterior boarder of the NAcSh in each section near the densest area of afferent IL fiber bundles.

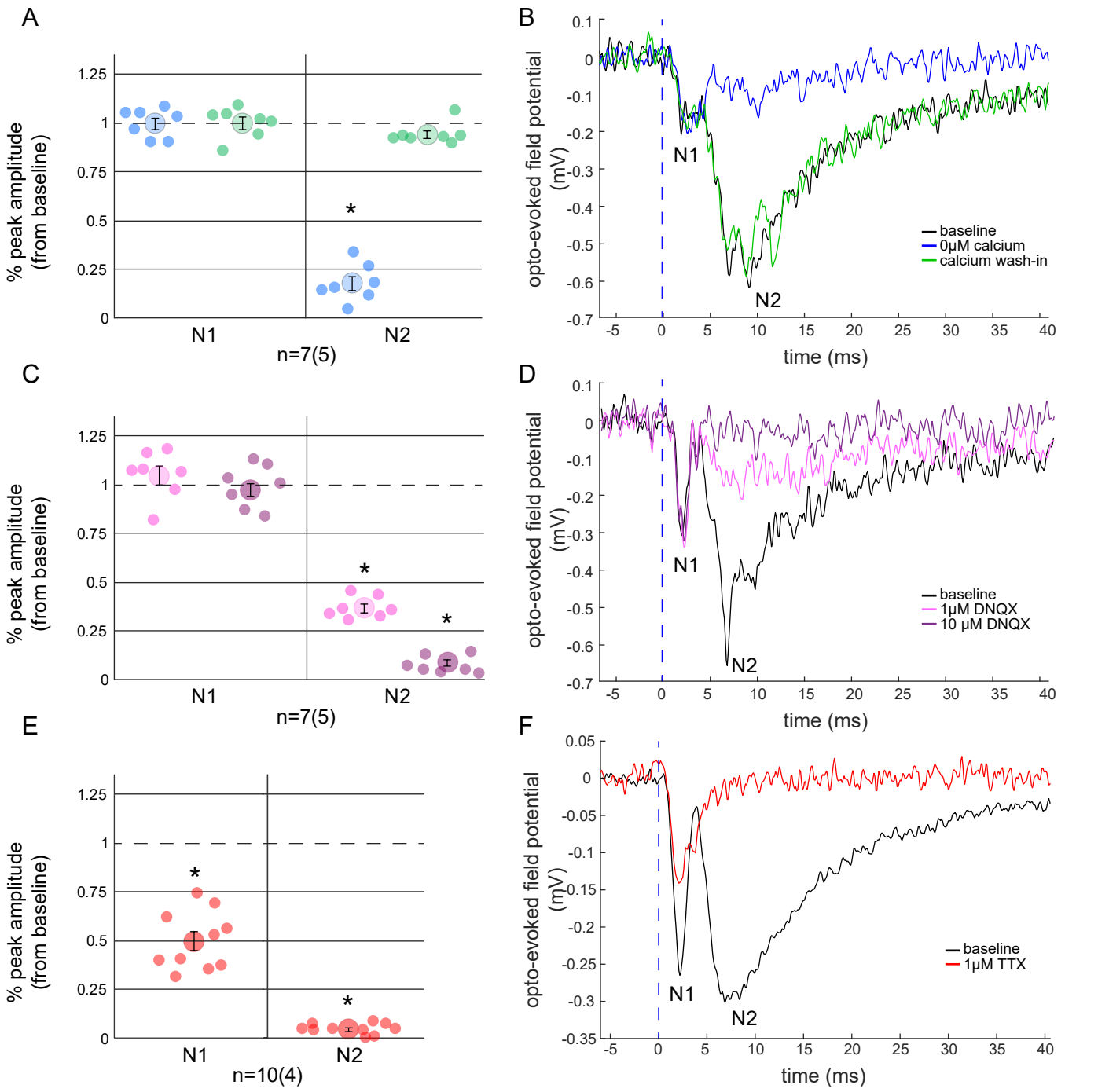

Figure S3. Pharmacological characterization of pre- and post-synaptic components of optogenetic evoked IL-NAcSh field potentials. Brief light pulse (1 ms) evoked a bimodal field potential waveform without eliciting a stimulus artifact recorded extracellularly in NAcSh slices. First and second negative peaks were labeled N1 and N2 respectively. Vertical dashed blue line represents onset of light pulse at time zero. (A-B) Switch to a 0μM calcium bath reduced only the peak N2 amplitude component without affecting the N1 component. N2 component was rescued following calcium wash-in. (C-D). Application of increasing bath concentrations of DNQX (AMPA receptor antagonist) reduced only the N2 component in a dose-dependent manner without affecting the N1 component. (E-F) Application of TTX (voltage-gated sodium channel antagonist) abolished the N2 component while reducing the N1 component. Peak amplitude was averaged from 25 pulses on a given slice and normalized to baseline peak averages. Dots in (A,C,E) represent individual slices. Sample size is noted on x-axis, with slice number followed by mouse number in parentheses. Larger dots represent mean +/- 1 standard error. *p<0.0001.

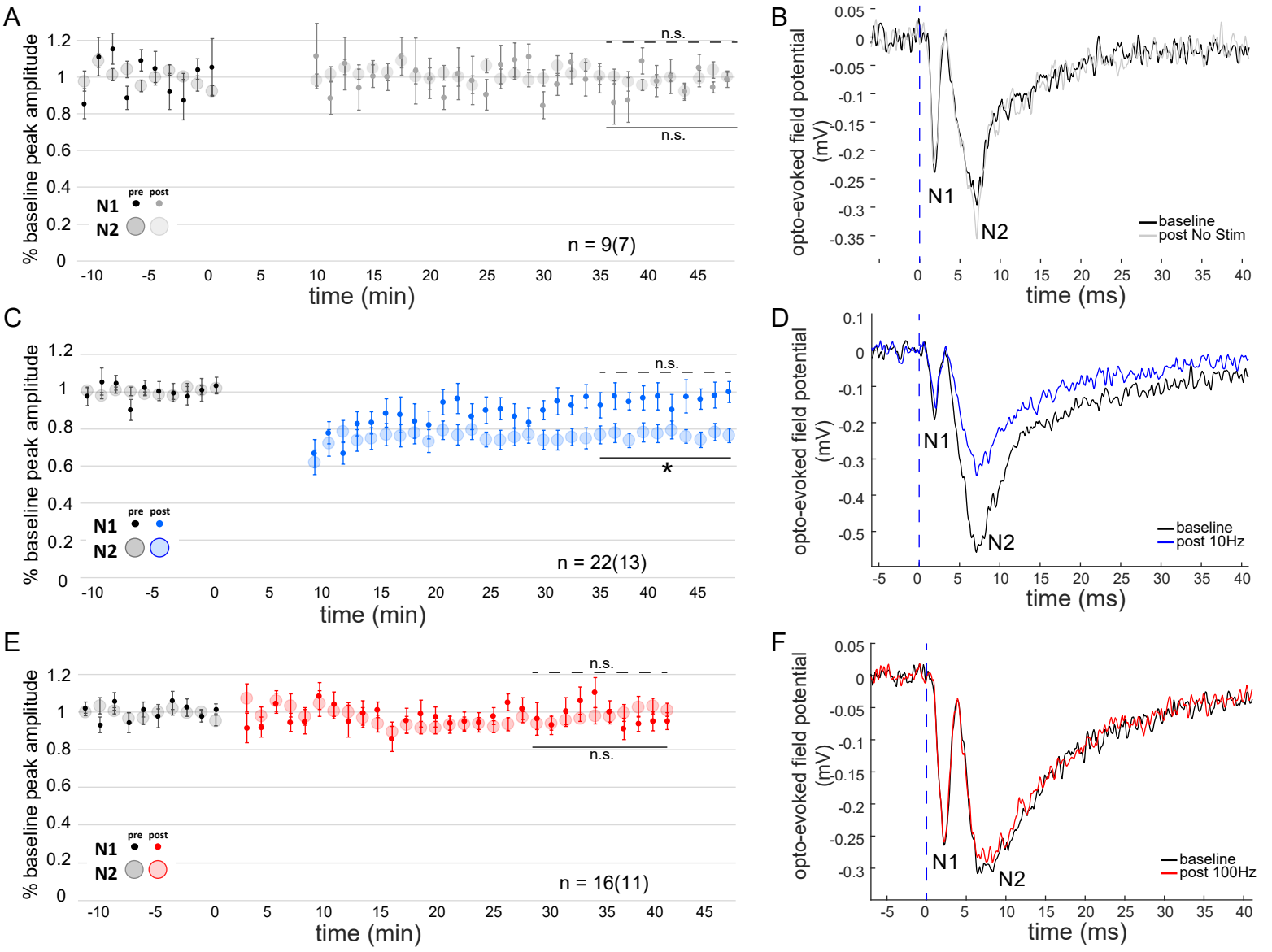

Figure S4. Assaying optogenetic-driven induction of plasticity in IL-NAcSh optogenetic evoked field potentials. Recordings were sampled at regular fixed intervals every 15 s. Peak N1 and N2 amplitudes were calculated from an average of 5 waveforms plotted every 1.25 min. After 12.5 min of recording baseline (50 waveforms yielding 10 average points), at time zero, slices were either exposed to 10min of no stimulation (A-B), a 10 Hz protocol (C-D) or a 100 Hz protocol (E-F). Regular sampling then resumed immediately after protocols ended for an additional 37.5 min (150 waveforms yielding 30 average points). Only the 10 Hz protocol induced long-term depression in the N2 component without eliciting a lasting effect on the N1 component. No changes were observed in either the N1 or N2 components in either the no stimulation or 100 Hz conditions. Sample size is noted above x-axis, with slice number followed by mouse number in parentheses. Plotted dots represent group mean across slices +/- 1 standard error. Example waveform traces plotted in (B,D,F) taken from an average of 50 baseline pulses and of the final 50 pulses. *p<0.0001, not significant (n.s.).

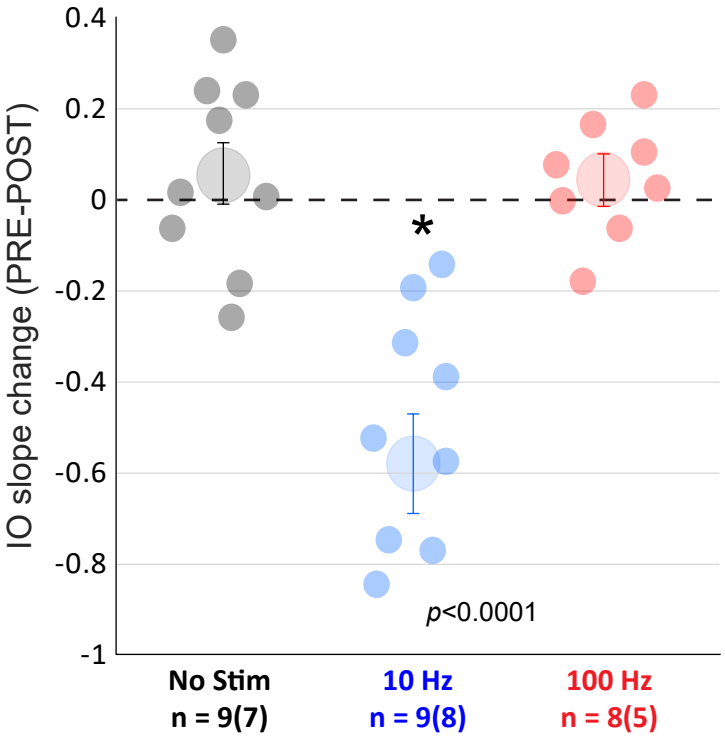

Figure S5. Optogenetic IO slope assay collected PRE and POST bath-application of plasticity-inducing protocols. Change in input-output assay from Fig.1G. 10hz group IO slope significantly decreased from zero. Dots represent individual slices. Sample size is noted near the x-axis, with number of slices followed by number of mice in parentheses. Larger dots represent mean +/- 1 standard error.

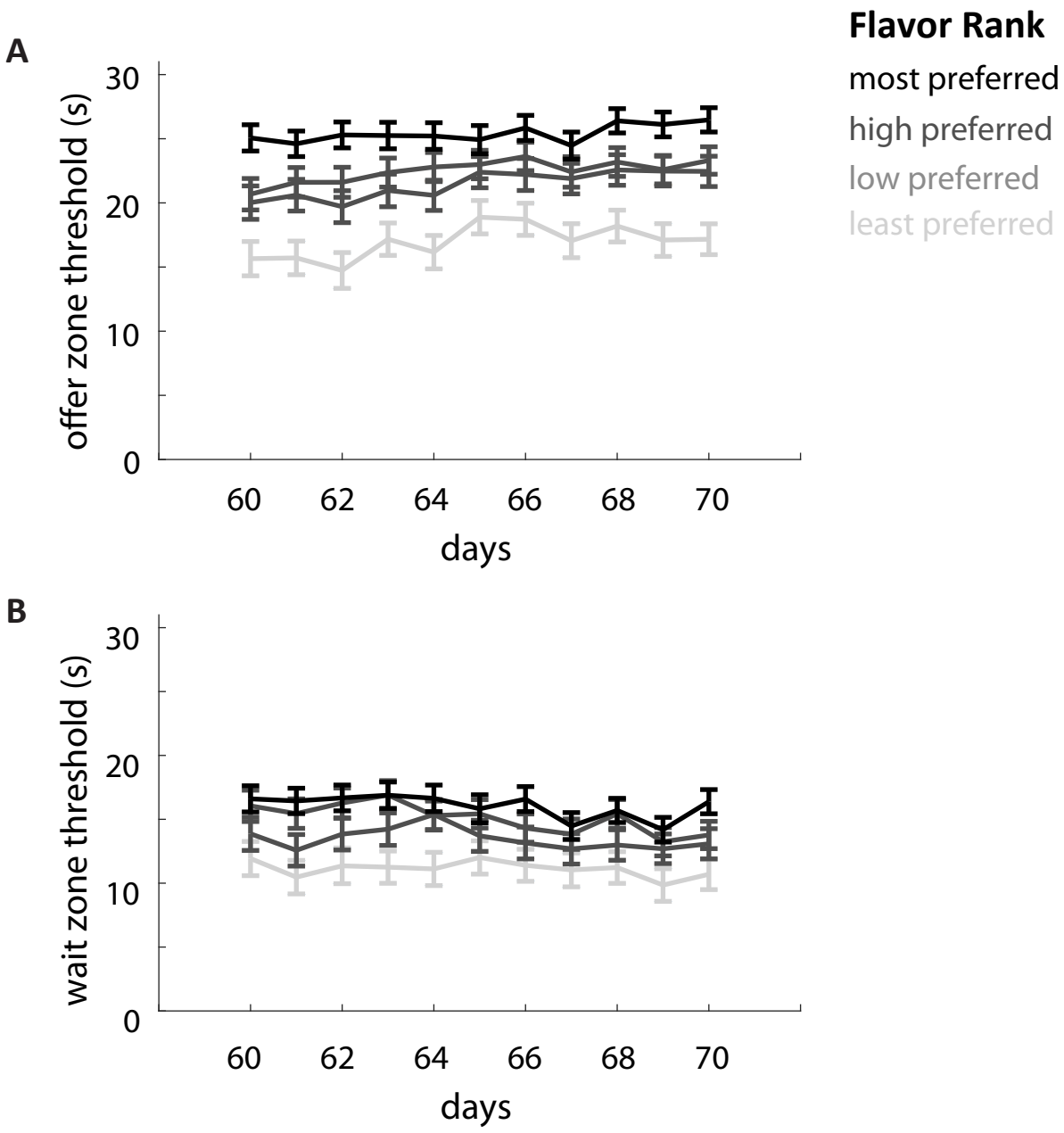

Figure S6. Stability of economic flavor preferences. Offer zone thresholds (A) and wait zone thresholds (B) were calculated for each day in well-trained mice (days 60-70). Flavor preference rankings were determined by calculating total pellets earned in a given restaurant summated across the entire 10 day window and ranked from least to most preferred. Data represent cohort (n=30) mean +/- 1 standard error.

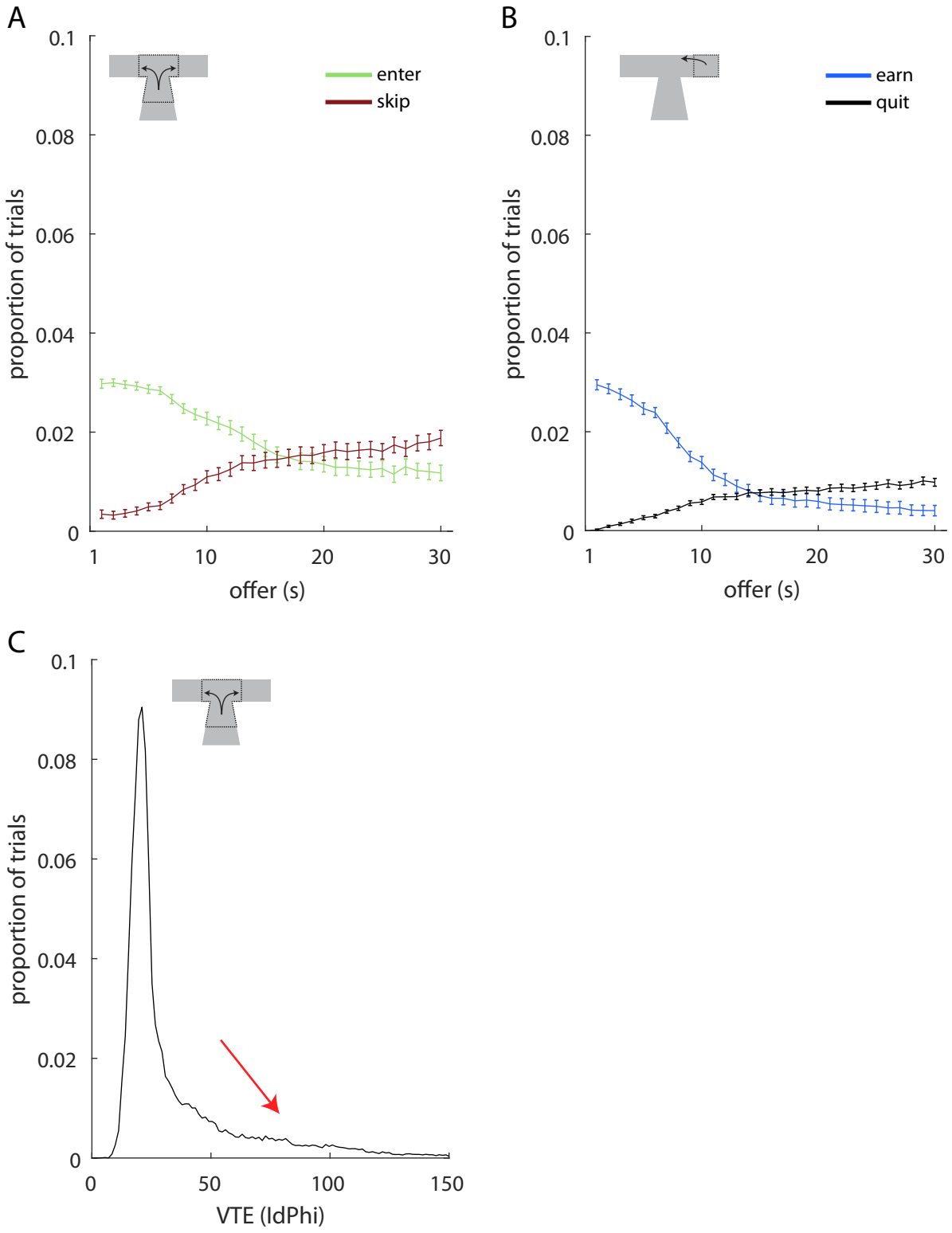

Figure S7. Economic choices and deliberative behaviors in the offer and wait zones. Data taken from 10 days of baseline (days 60-70) from all 30 mice. (A) Offer zone choice probability between skipping vs. entering as a function of offer length. Mice entered low delay offers and skipped high delay offers based on cue tone pitch presented at trial onset (restaurant entry). (B) Wait zone choice probability between quitting during the countdown vs. earning as a function of offer length. Plotted lines represent group mean across mice +/- 1 standard error. (C) In the offer zone, mice displayed “pause and look” behaviors, known as “vicarious trial and error” (VTE).(35-37) VTE reveals on-going deliberation and planning during moments of indecision, supported by numerous electrophysiological experiments.(35-37) VTE is measured as the absolute integrated angular velocity (in IdPhi units) calculated from the animal’s X-Y-location path-trajectory measured from offer onset until either a skip or enter decision is made. The right-tailed shape (red arrow) of the distribution of IdPhi reflect population of trials with increasing deliberative behaviors during moments of indecision.

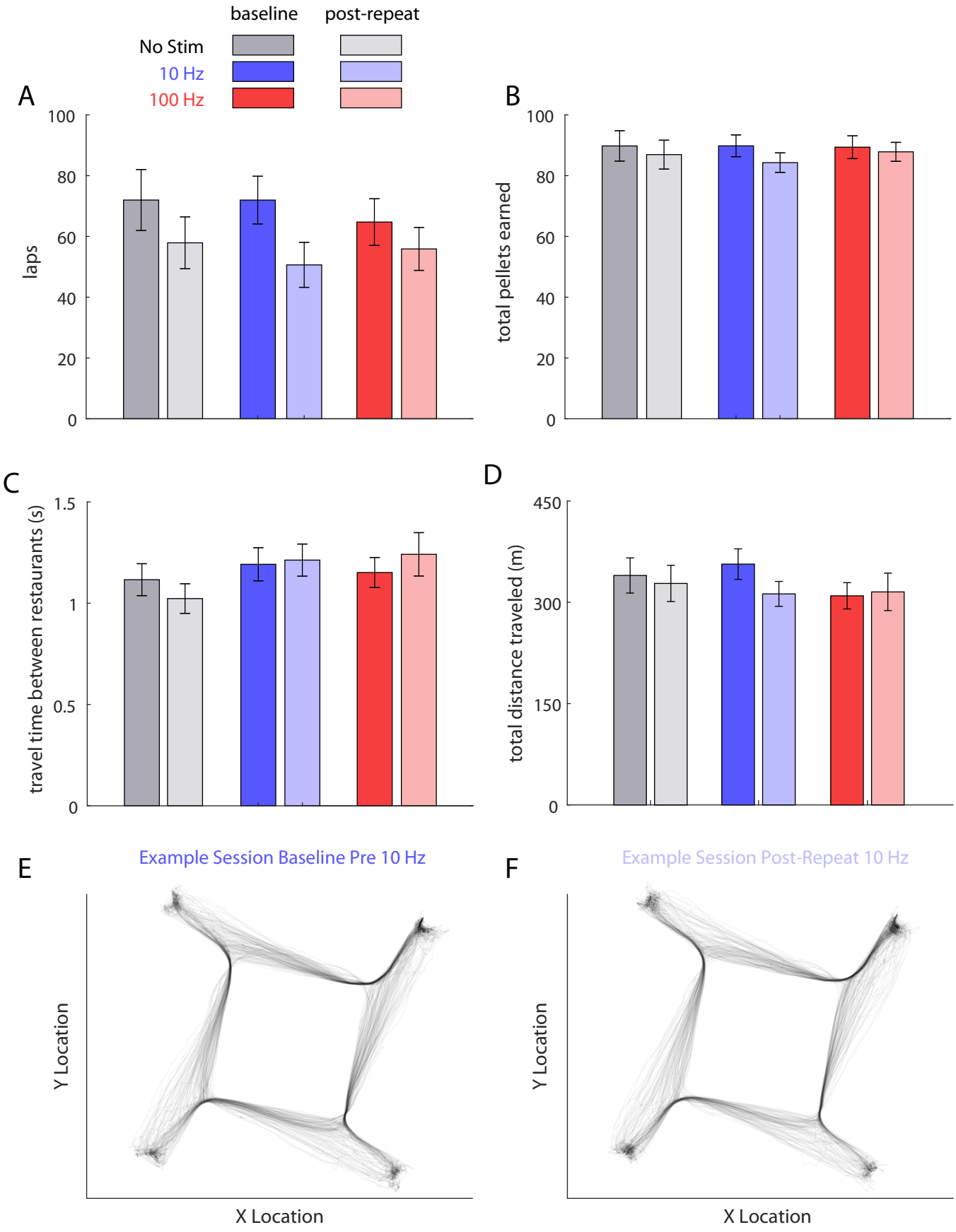

Figure S8. Controlling for non-specific appetitive or locomotor abilities before and after optogenetic manipulations. No changes were observed in total number of laps run (A), total number of food pellets earned (B), or locomotor ability (C-F, travel speed or distance traveled) comparing 9 days before the first round of optogenetic stimulation (baseline) and 9 days following round 3 of optogenetic stimulation (post-repeat stimulations, when robust wait zone decision-making changes were observed). Plotted bars represent group mean (n=10 per group) across mice +/- 1 standard error. Track plots in (E-F) depict an example testing session X-Y body tracking positions of a mouse displayed across the entire 1hr session.

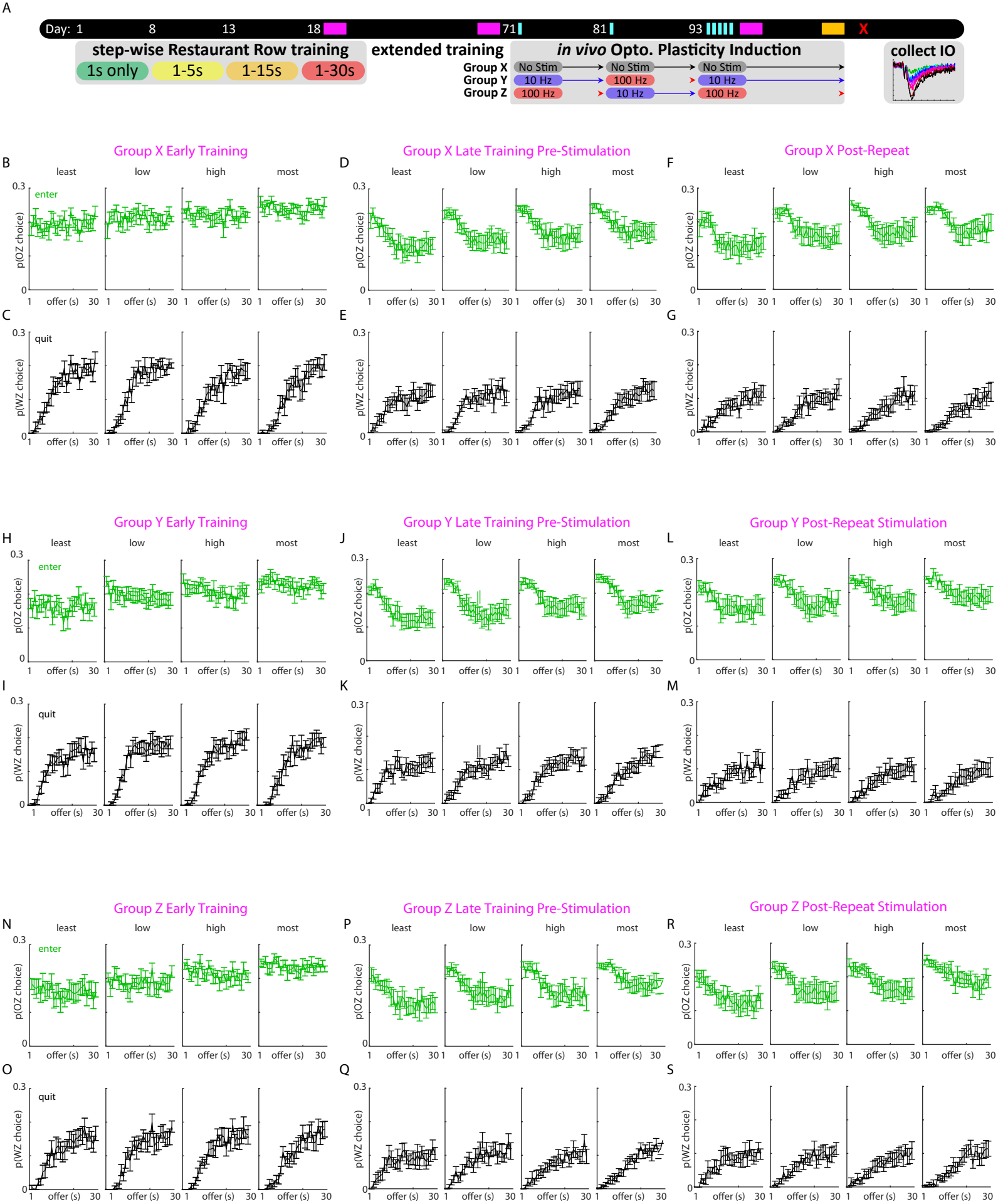
A
Day: 1
8
13
18
71
81
93
X
step-wise Restaurant Row training
1s only
1-5s
1-15s
1-30s
extended training
in vivo Opto. Plasticity Induction
Group X
Group Y
Group Z
No Stim
10 Hz
100 Hz
collect IO
Group X Early Training
Group X Late Training Pre-Stimulation
Group X Post-Repeat
Group Y Early Training
Group Y Late Training Pre-Stimulation
Group Y Post-Repeat Stimulation
Group Z Early Training
Group Z Late Training Pre-Stimulation
Group Z Post-Repeat Stimulation
least
low
high
most
enter
quit
p(OZ choice)
p(WZ choice)
offer (s)

Figure S9. Controlling for learned spatial task rules before and after optogenetic manipulations. (A) Experimental timeline. Three windows of time marked by magenta blocks indicate early training in the 1-30s environment (days 18-22, B-C,H-I,N-O), late training (days 66-70, D-E,J-K,P-Q), and post-repeat stimulation (days 98-102, F-G,L-M,R-S). (B-S) Offer zone (probability of entering) and wait zone decisions (probability of quitting) depicted as a function of offer cued offer length randomly selected on each trial split by subjective flavor preference rankings (least preferred to most preferred). Experimental treatment conditions are labeled by Groups X, Y, and Z in timeline (A) and throughout (B-S). Early in training (first magenta block, B-C,H-I,N-O), all animals made offer zone decisions to enter depending on subjective flavor preferences (entered more in higher preferred restaurants, $F=11.74$, $p<0.0001$) but with no regard to offer length ($F=1.53$, $p=0.16$). This indicates cued tone information was not incorporated into offer zone decisions and economic behaviors relied solely on wait-zone quit decisions. By late in training (second magenta block, D-E,J-K,P-Q), all animals learned to discriminate randomly presented offer lengths in the offer zone while still ascribing different subjective values to those offers depending on flavor preferences ($F=5.33$, $p<0.01$, restaurant identity communicated through visuospatial cues). Following the stimulation protocols (third magenta block, F-G,L-M,R-S), all animals retained the ability to discriminate randomly presented cued costs in the offer zone while still ascribing subjective value through learned spatial relationships ($F=5.22$, $p<0.01$), but there were no differences between experimental groups ($F=0.29$, $p=0.94$).

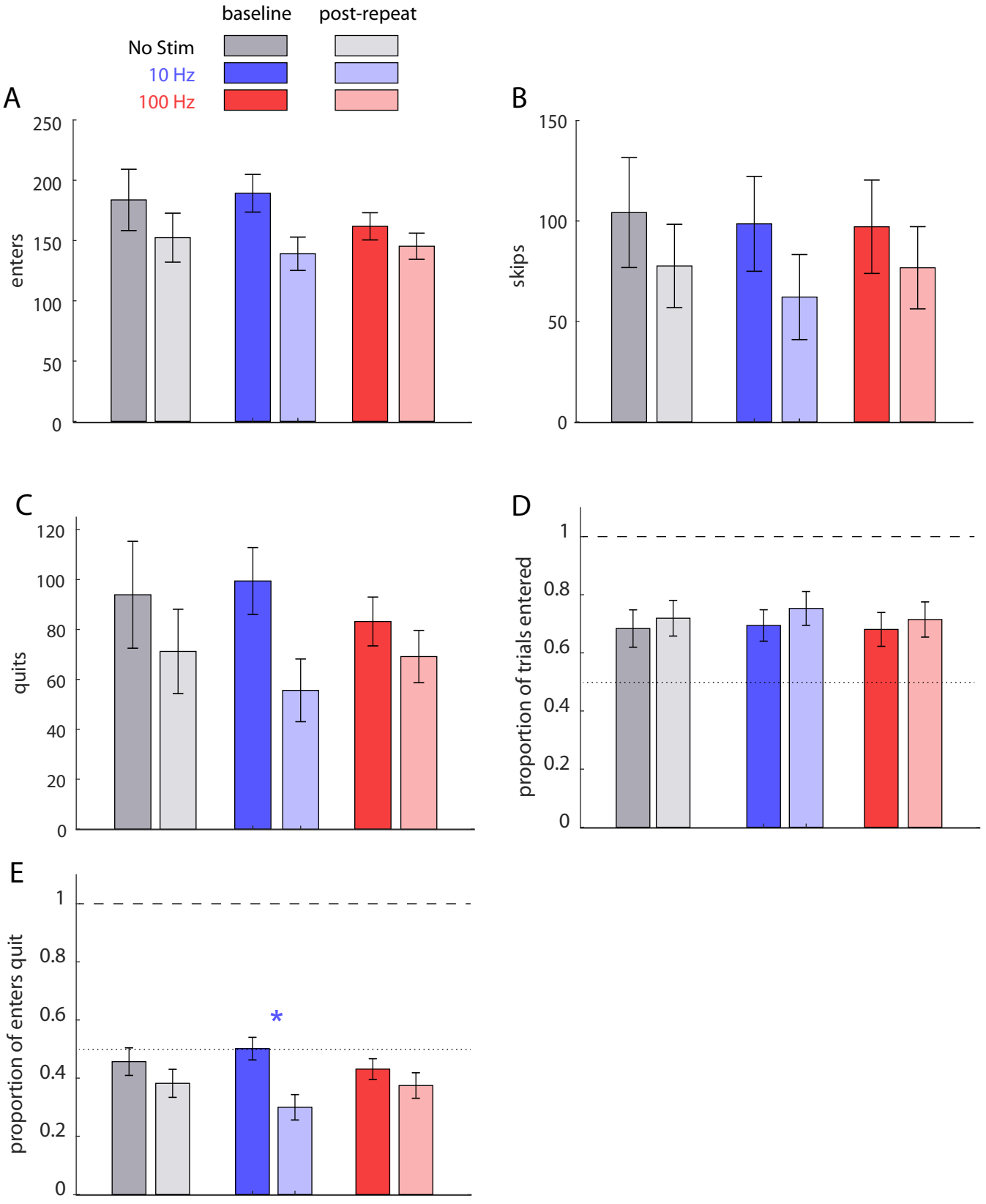

Figure S10. Restaurant Row quantification of decision types before and after optogenetic manipulations. **(**A-C) No changes were observed in total number enter decisions (A, F=2.11, p=0.14), total number of skip decisions (B, F=0.21, p=0.82), or total number of quit decisions (C, F=2.90, p=0.07). (D) Normalizing number of offer zone decisions to total number of laps run, no changes were observed in proportion of trials that were entered (F=0.15, p=0.86). (E) However, normalizing number of wait zone decisions to total number of offers entered, only the 10 Hz group showed a significant decrease in proportion of enter decisions that were then quit (F=5.94, p<0.01, post-hoc Tukey comparisons: baseline 10 Hz vs. post-repeat 10 Hz, t=6.22, p<0.0001, baseline No Stim vs. post-repeat No Stim, t=2.3, p=0.23, baseline 100 Hz vs. post-repeat 100 Hz, t=1.7, p=0.52). Plotted bars represent group mean (n=10 per group) across mice +/- 1 standard error. *p<0.0001.

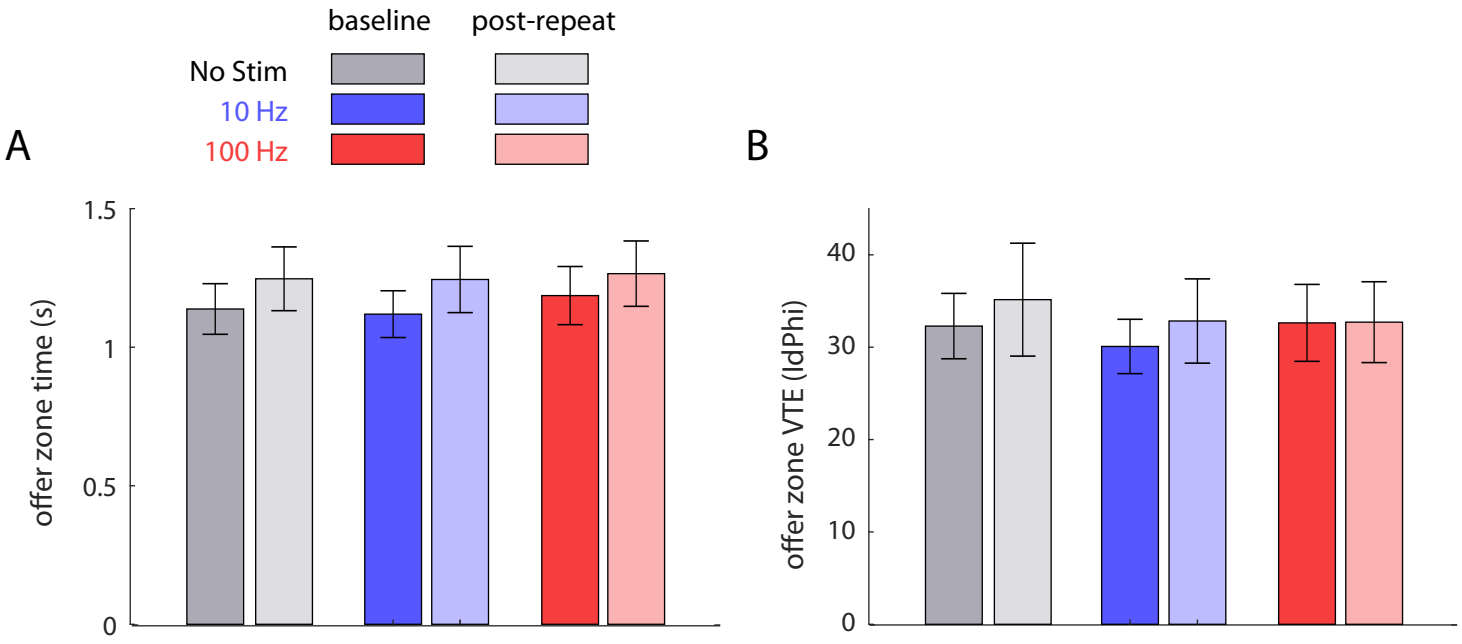

Figure S11. Restaurant Row offer-zone behaviors before and after optogenetic manipulations. (A-B) No changes were observed in offer zone reaction time (A, F=0.16, p=0.86) or offer zone VTE behavior (B, F=0.28, p=0.76). Plotted bars represent group mean (n=10 per group) across mice +/- 1 standard error.

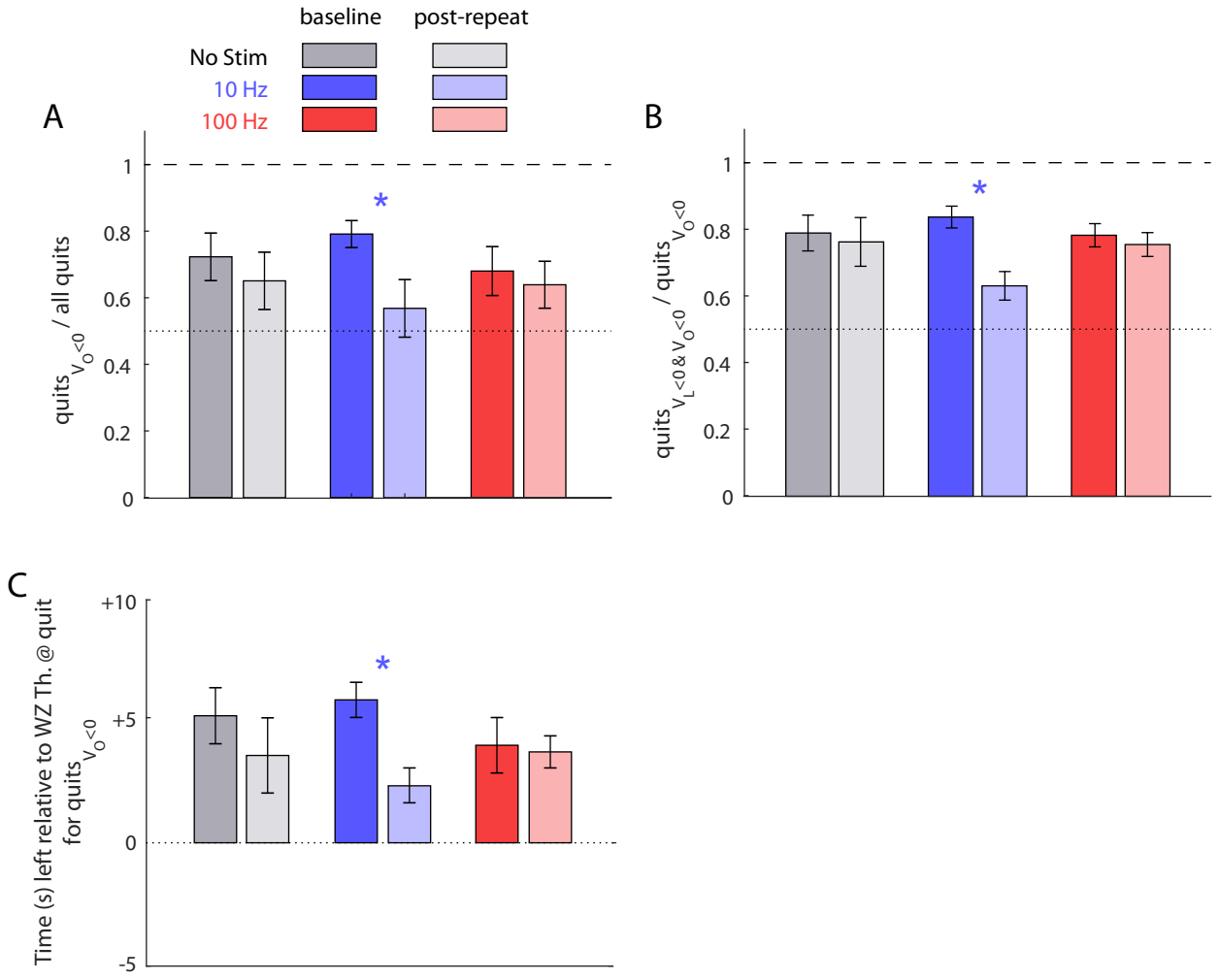

Figure S12. Restaurant Row wait-zone behaviors before and after optogenetic manipulations. We quantified the value (V) of a reward offer (O) normalized to subjective economic preferences for each individual and each restaurant within each session by subtracting the offer length from each respective wait zone threshold (VO=WZ th. – offer). Thus, offers where VO<0 reflect negatively valued offers ("bad" deals) where the delay was greater than what mice were typically willing to wait for and earn. (A) We calculated the proportion of quit events where VO<0 relative to all quits and found that the majority of quits for all mice at baseline were for "bad" deals, correcting offer zone decisions of low value (high delay, high cost) that mice had initially accepted. However, only the 10 Hz group showed a significant reduction ($F=3.84$, $p<0.05$, post-hoc Tukey comparisons: baseline 10 Hz vs. post-repeat 10 Hz, $t=4.57$, $p<0.01$, baseline No Stim vs. post-repeat No Stim, $t=1.5$, $p=0.65$, baseline 100 Hz vs. post-repeat 100 Hz, $t=0.9$, $p=0.94$). (B) We then measured the amount of time left remaining in the countdown at the moment mice made quit decisions and calculated the value of time left (VL) relative to wait zone thresholds (VL=WZ th. – time left). Example: a mouse with a 15 s wait zone threshold accepts a 25 s offer and then quits after 5 s of waiting in the wait zone with 20 s left remaining in that trial's countdown. Thus VO=-10 and VL=-5 on this example trial. Therefore, trials where VO<0 and VL<0 reflect "bad" deals that were initially accepted in the offer zone but were quit in the wait zone while the remaining investment required was still a "bad" deal. We calculated the proportion of "bad" deals that were accepted that were quit in an economically efficient manner where deals were still "bad" when quitting and found that all mice at baseline quit in an economically efficient manner on the majority of "bad" deal quits, truly re-evaluating and changing their minds to correct initial offer zone decisions to enter on these trials. However, only the 10 Hz group showed a significant reduction in economic efficiency of "bad" deal quits ($F=3.39$, $p<0.05$, post-hoc Tukey comparisons: baseline 10 Hz vs. post-repeat 10 Hz, $t=3.68$, $p<0.05$, baseline No Stim vs. post-repeat No Stim, $t=0.5$, $p=0.99$, baseline 100 Hz vs. post-repeat 100 Hz, $t=0.5$, $p=0.98$). (C) Lastly, we calculated the average number of seconds relative to wait zone threshold that were remaining in the countdown at the moment of quitting "bad" offers and found that all mice at baseline, across all trials, quit when the time left was above wait zone thresholds by approximately 5s, consistent with the notion in (B). However, only in the 10 Hz group we found a significant reduction ($F=4.14$, $p<0.05$, post-hoc Tukey comparisons: baseline 10 Hz vs. post-repeat 10 Hz, $t=4.23$, $p<0.01$, baseline No Stim vs. post-repeat No Stim, $t=0.5$, $p=0.99$, baseline 100 Hz vs. post-repeat 100 Hz, $t=1.0$, $p=0.91$). Plotted bars represent group mean (n=10 per group) across mice +/- 1 standard error. *$p<0.01$.

Table S1. Statistical report of Fig. 3H-J. Two-way repeated measures ANOVA was run comparing stimulation condition against time points between stimulation rounds. Interaction effects are reported as well as post-hoc between-group and within-group, across time tests corrected for multiple comparisons. Green text indicates significant findings.

Statistical test			Stimulation Round 1	Stimulation Round 2	Stimulation Round 3
ANOVA stim. x days			F=4.58, p<0.05	F=4.10, p<0.05	F=14.05, p<0.0001
	Tukey post-hoc: baseline stim vs. **post no stim**		t=-1.6, p=0.61	t=-0.5, p=0.60	t=-1.7, p=0.56
	Tukey post-hoc: baseline 10 Hz vs. **post 10 Hz**		t=-5.7, p<0.0001	t=-4.22, p<0.0001	t=-7.1, p<0.0001
	Tukey post-hoc: baseline 100 Hz vs. **post 100 Hz**		t=-2.4, p=0.12	t=-1.0, p=0.34	t=0.09, p=0.99
		Tukey post-hoc: **post no stim** vs. **post 10 Hz**	t=-3.3, p<0.05	t=-2.3, p<0.05	t=-3.7, p<0.01
		Tukey post-hoc: **post no stim** vs. **post 100 Hz**	t=-0.8, p=0.96	t=-0.3, p=0.78	t=1.2, p=0.84